Supplementary Information (SI) for Nanoscale Advances.
This journal is © The Royal Society of Chemistry 2025

# Electronic Supporting Information

## A pH-sensitive β-cyclodextrin-modified periodic mesoporous organosilica hybrid nanomaterial for co-delivery of paclitaxel and curcumin in lung cancer

Negin Rostami[a,b], Mohammad Reza Naimi-Jamal[a]*, Mohammad G. Dekamin[b]*

*a. Research Laboratory of Green Organic Synthesis and Polymers, Department of Chemistry, Iran University of Science and Technology, P.O. Box 16846–13114, Tehran, Iran.*

**Email: naimi@iust.ac.ir*

*b. Pharmaceutical and Heterocyclic Compounds Research Laboratory, Department of Chemistry, Iran University of Science and Technology, Tehran, 16846-13114, Iran.*

**Email: mdekamin@iust.ac.ir*

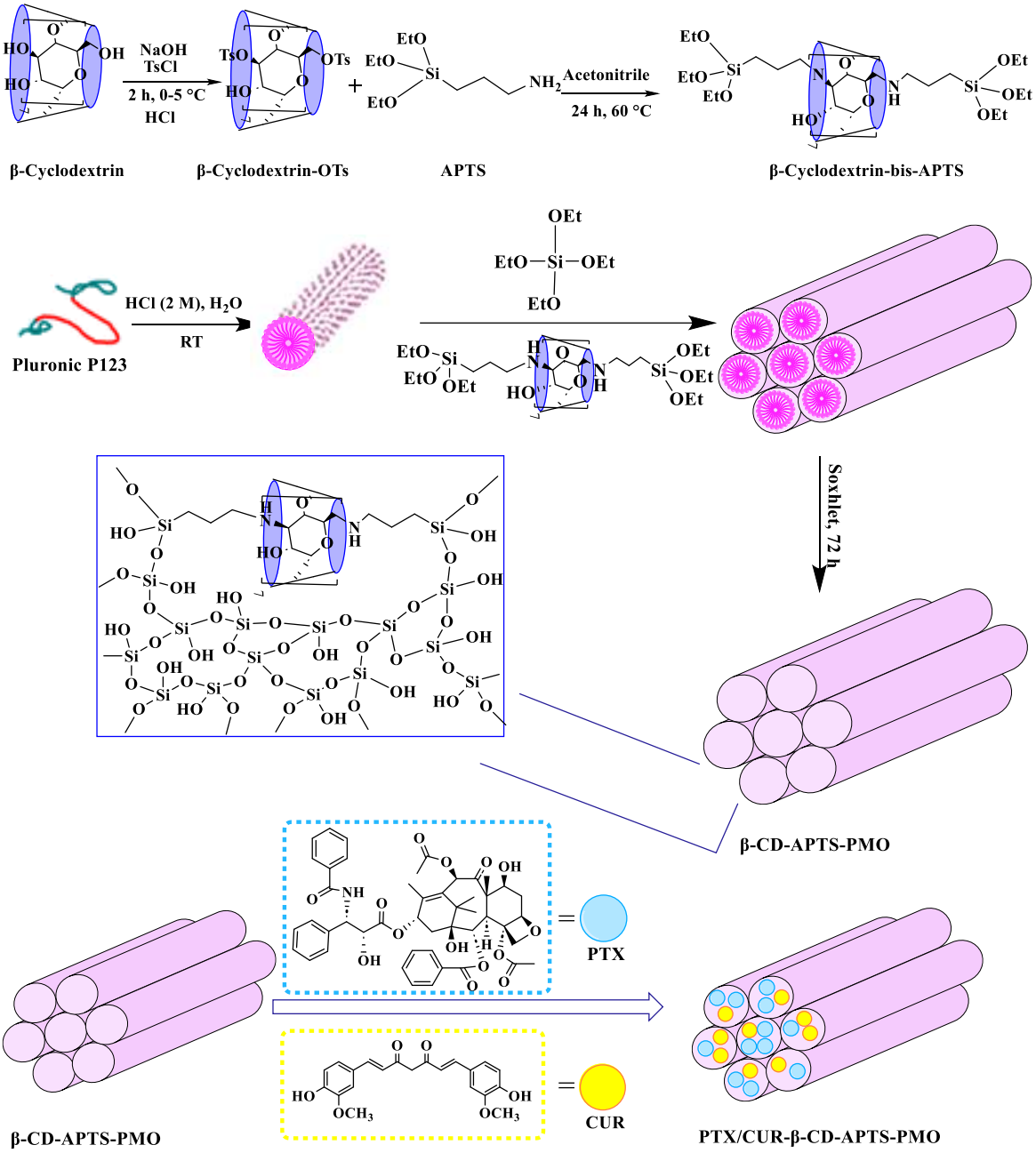


**Scheme 1** Schematic synthesis and fabrication process of β-CD-APTS-PMO and co-delivery of PTX and CUR.

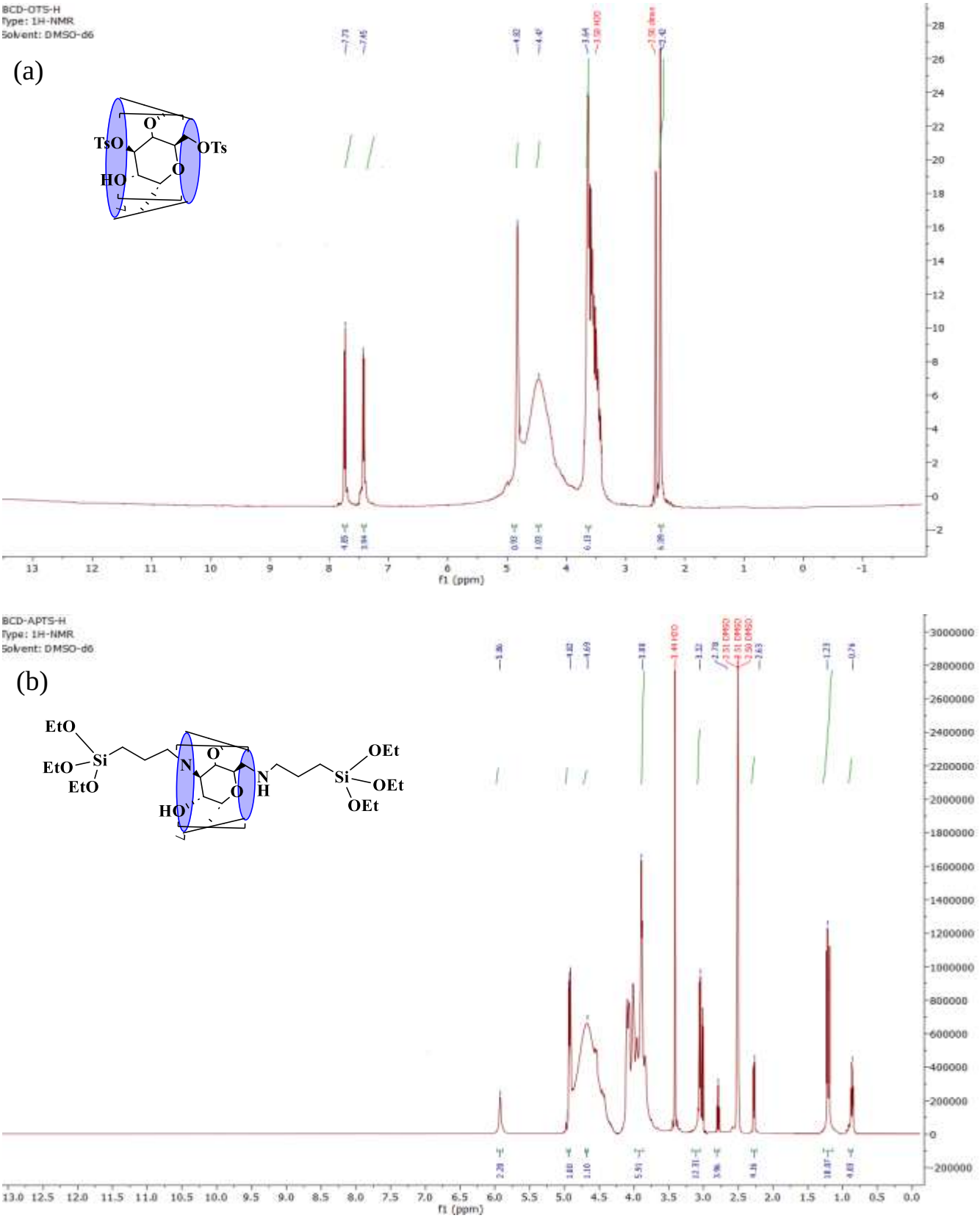


**Fig. 1** [1]HNMR of β-CD-OTs (a)and β-CD-bis-APTS (b)

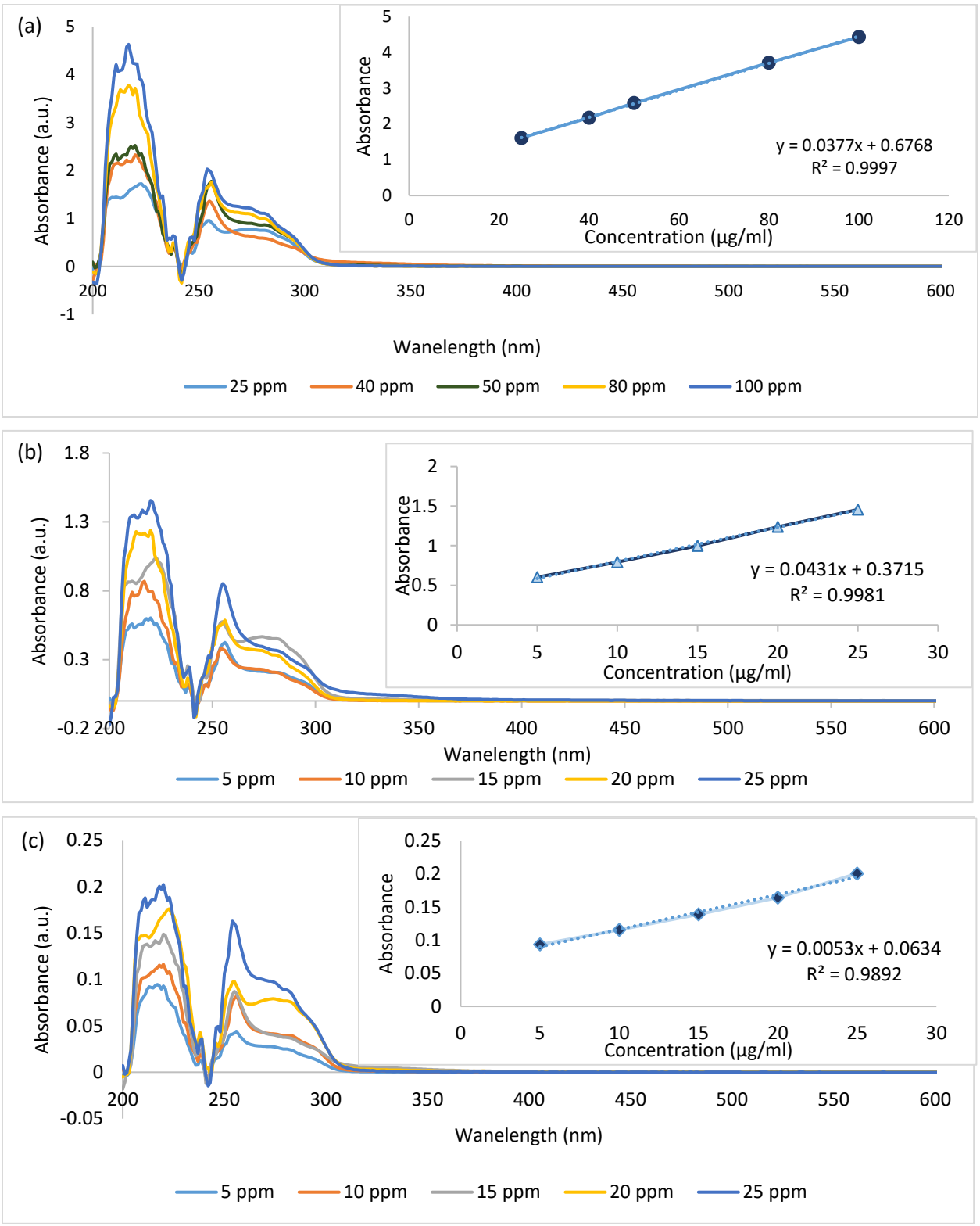


**Fig. 2** Calibration curve of paclitaxel in (a) ETOH, (b) Phosphate buffer pH 7.4 (c) Phosphate buffer pH 5.5

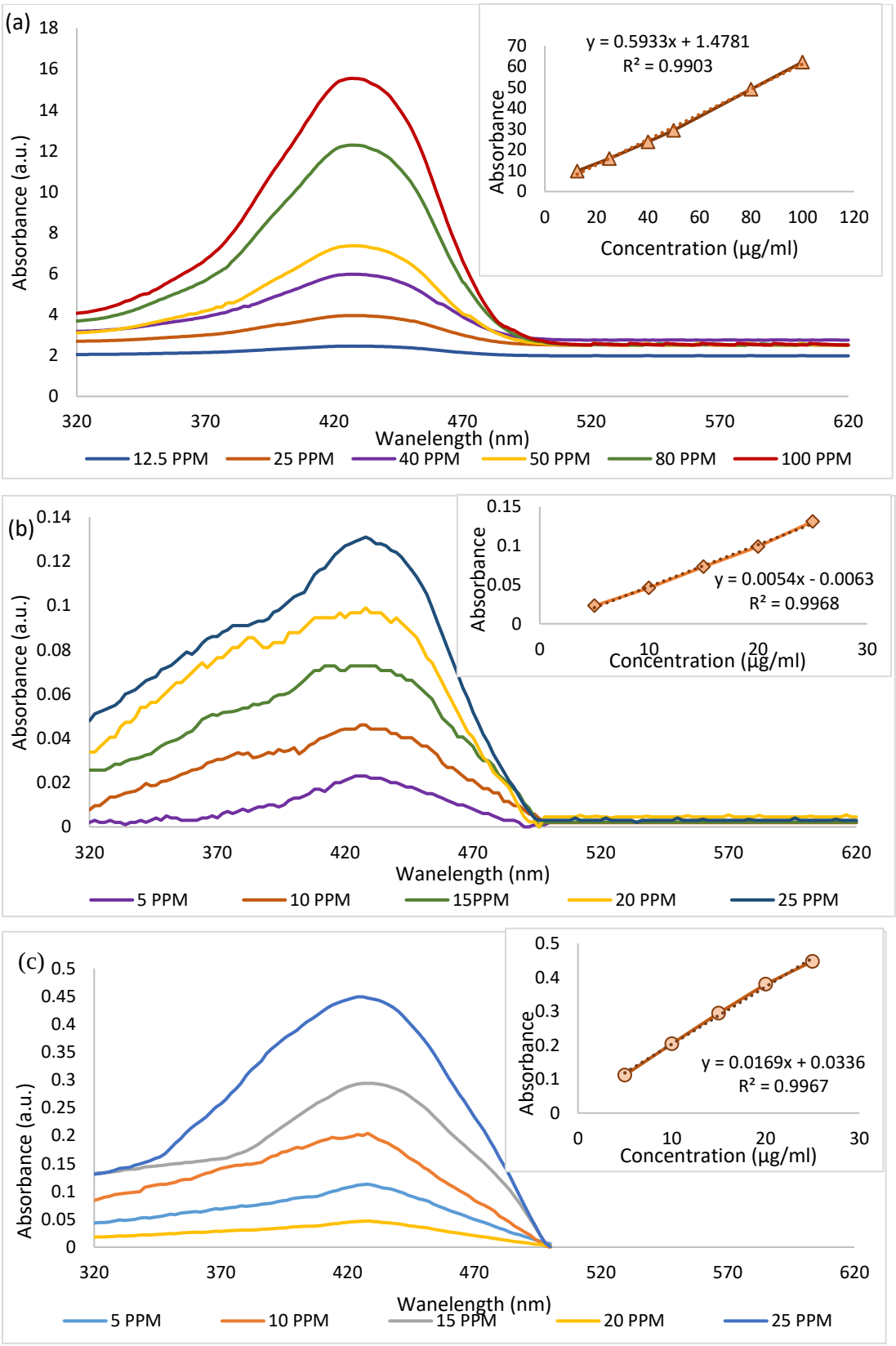


**Fig. 3** Calibration curve of curcumin in (a) ETOH, (b) Phosphate buffer pH 7.4 (c) Phosphate buffer pH 5.5

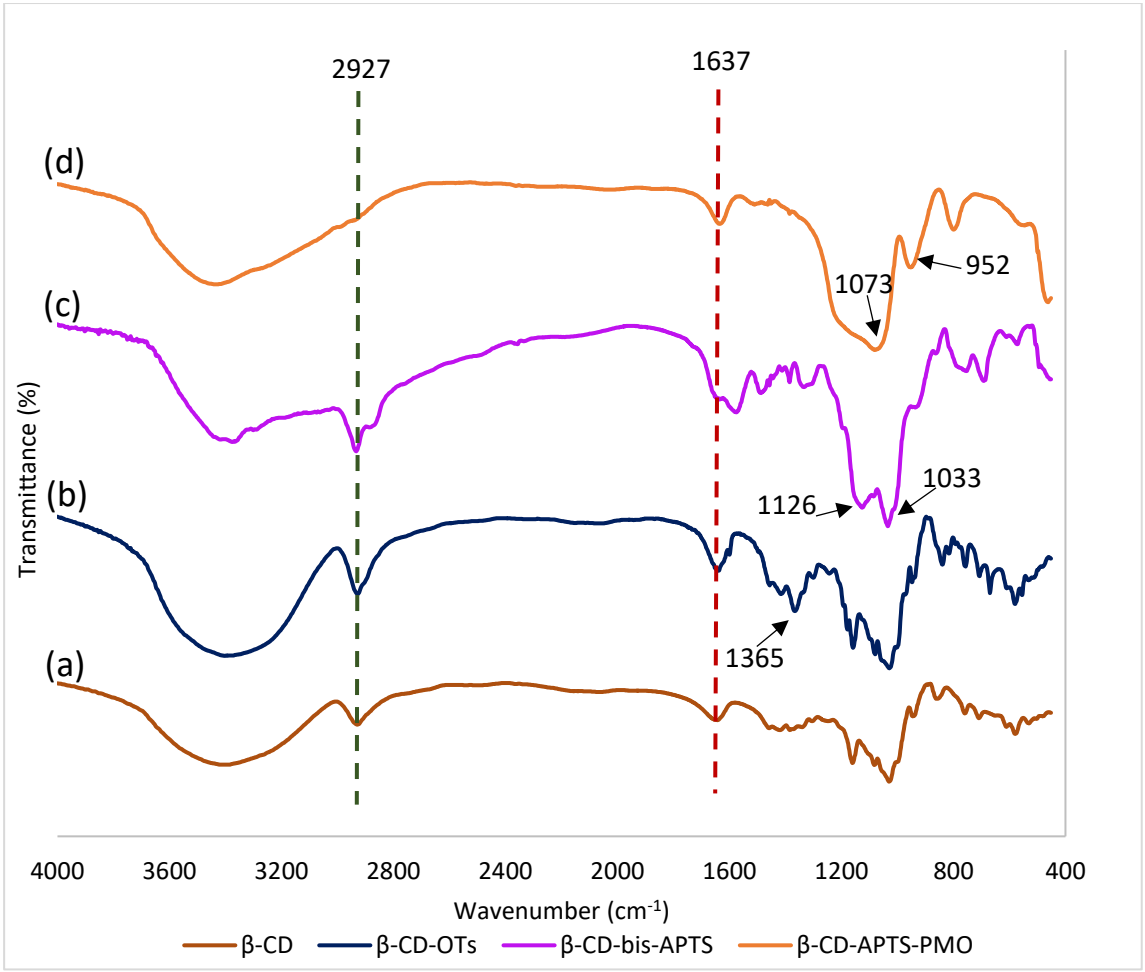


**Fig. 4** FTIR spectra of the β-CD (a), β-CD-OTs (b), β-CD-bis-APTS (c) and β-CD-APTS-PMO (d).

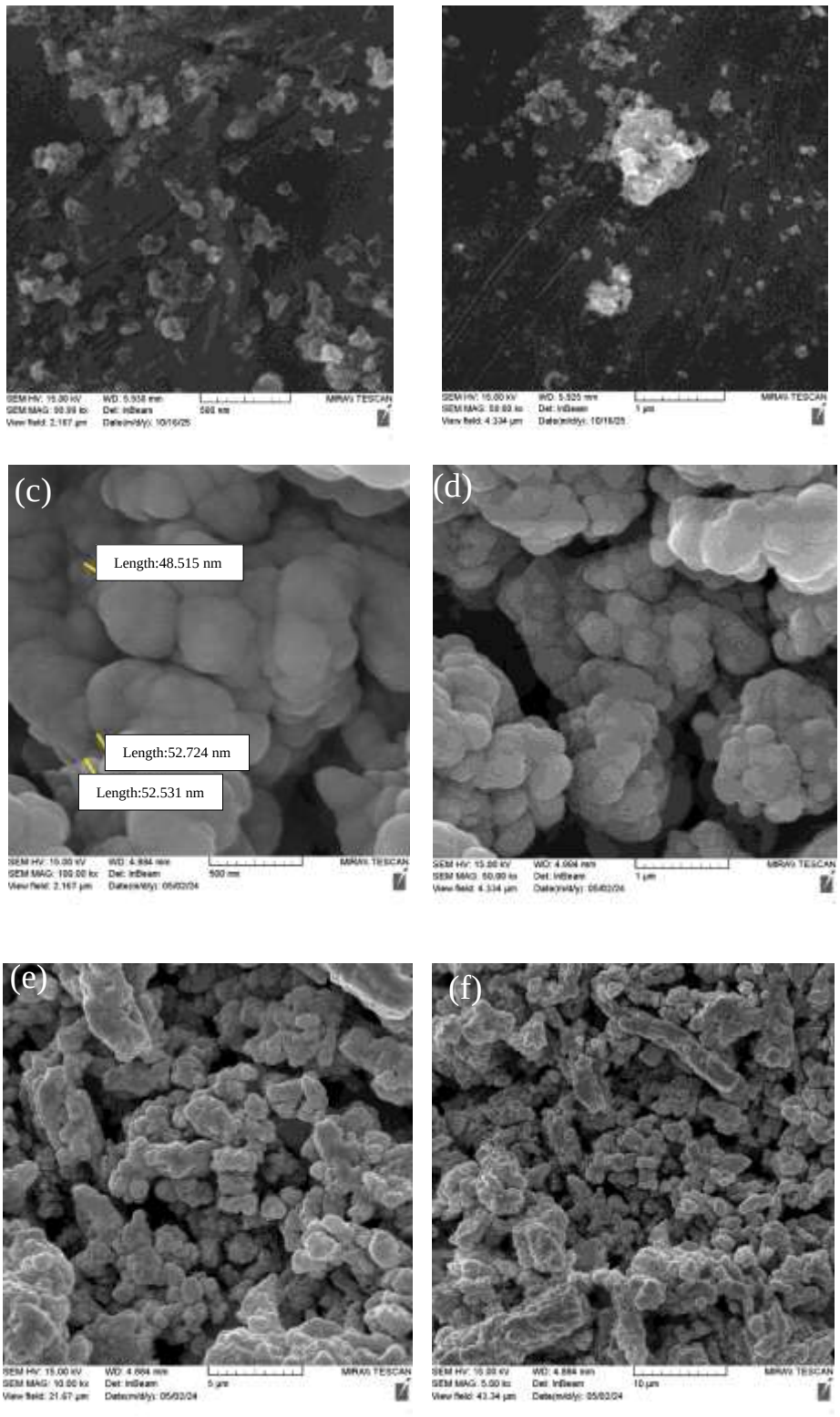


**Fig. 5** FESEM images of (a-b) β-CD-bis-APTS and (c-f) β-CD-APTS-PMO with different magnifications

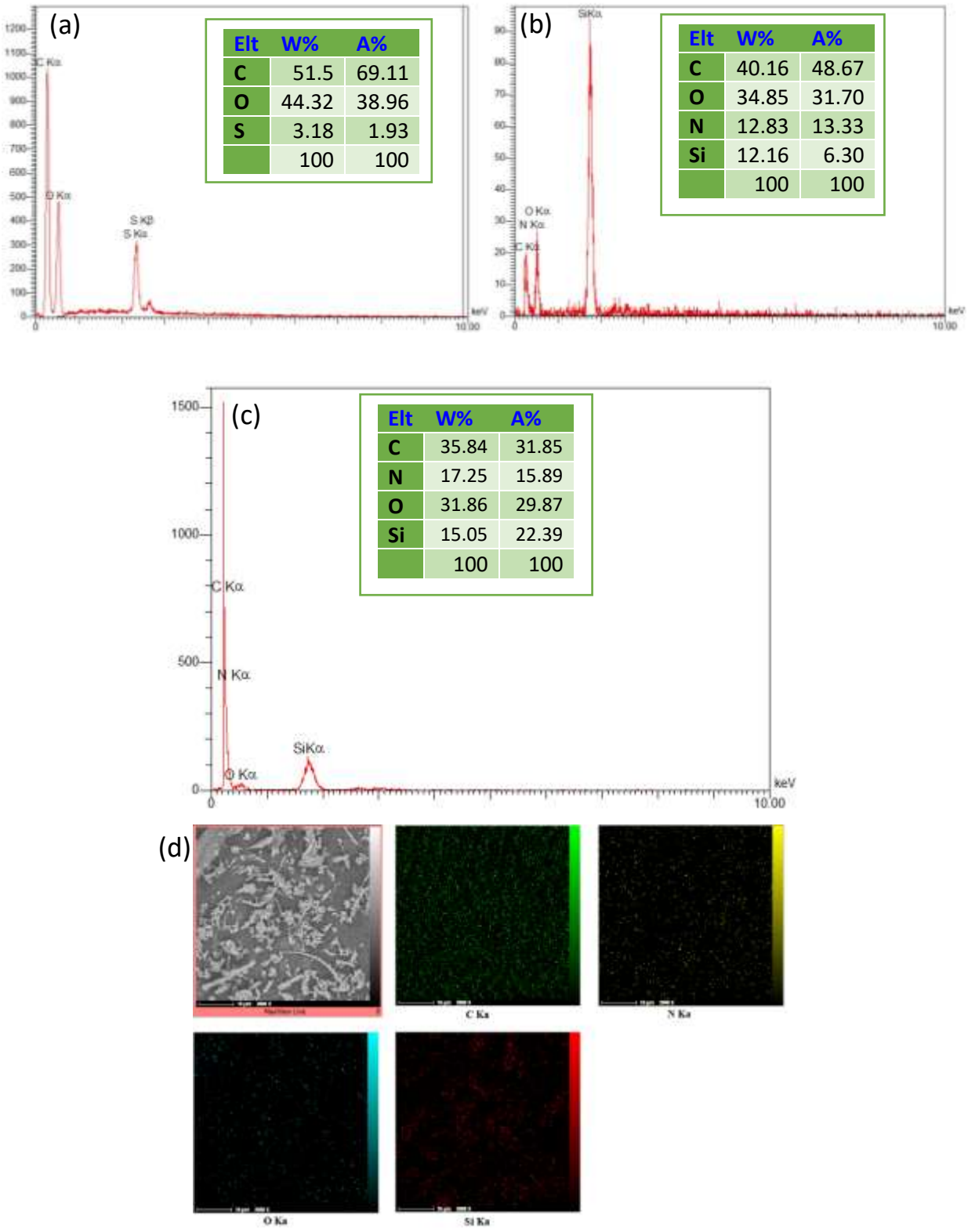


**Fig. 6** EDX analysis of β-CD-OTs (a), β-CD-bis-APTS (b) and β-CD-APTS-PMO (c) elemental mapping of β-CD-APTS-PMO (d)

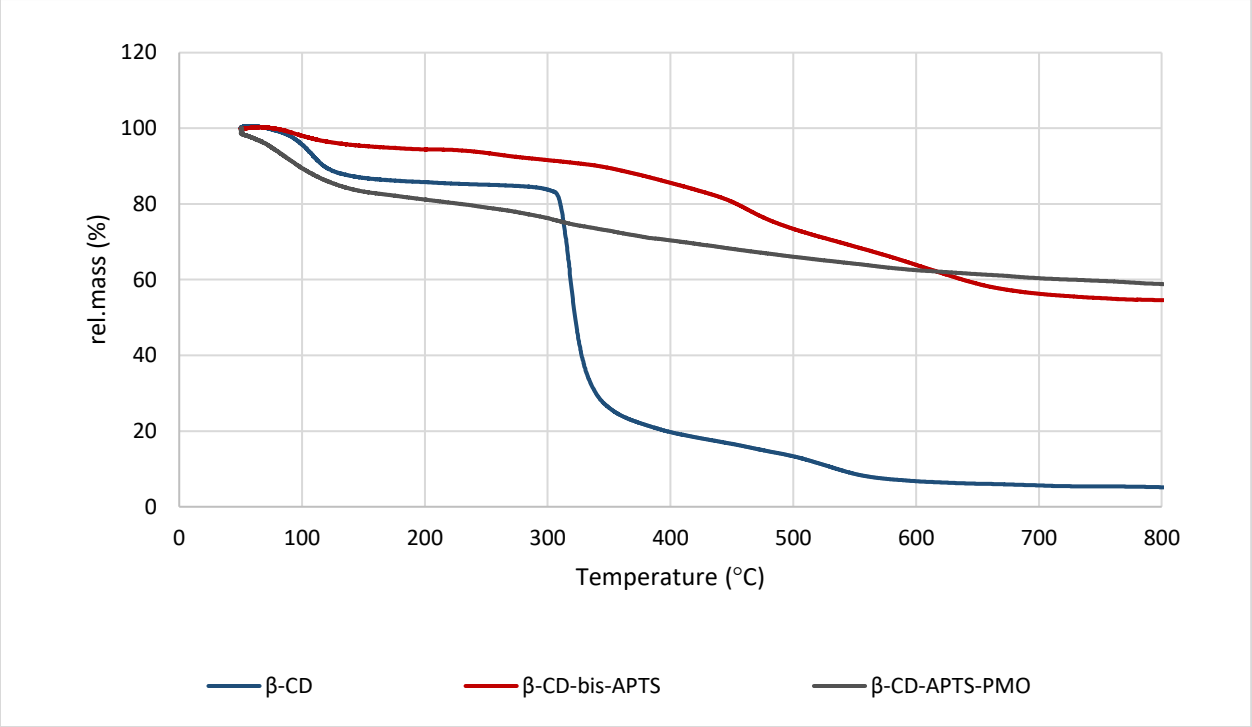


**Fig. 7** Thermogravimetric curve of the β-CD, β-CD-bis-APTS and β-CD-APTS-PMO.

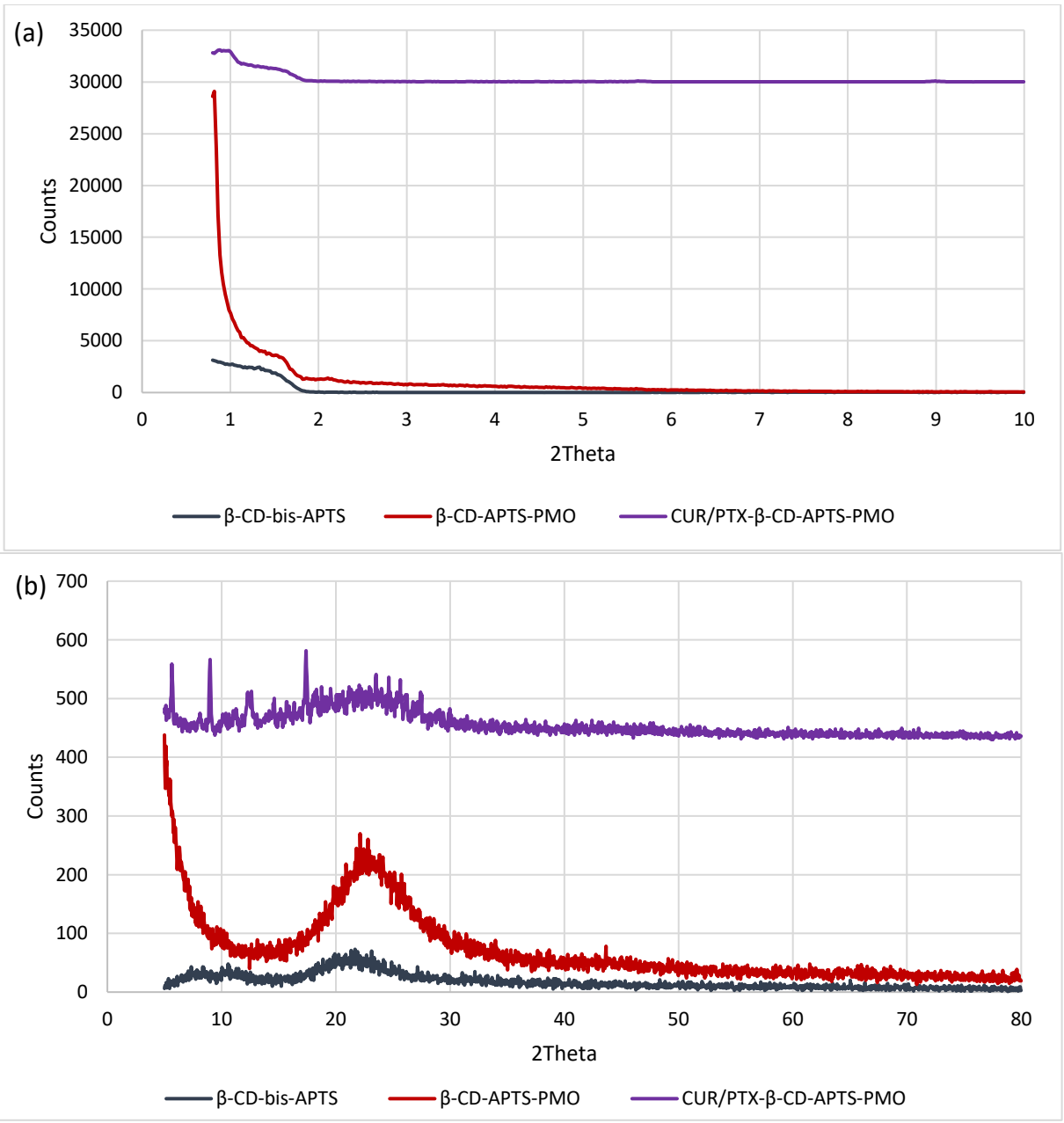


**Fig. 8** Low-angle (a) and wide-angle XRD pattern of the β-CD-bis-APTS, β-CD-APTS-PMO, CUR/PTX-β-CD-APTS-PMO (b).

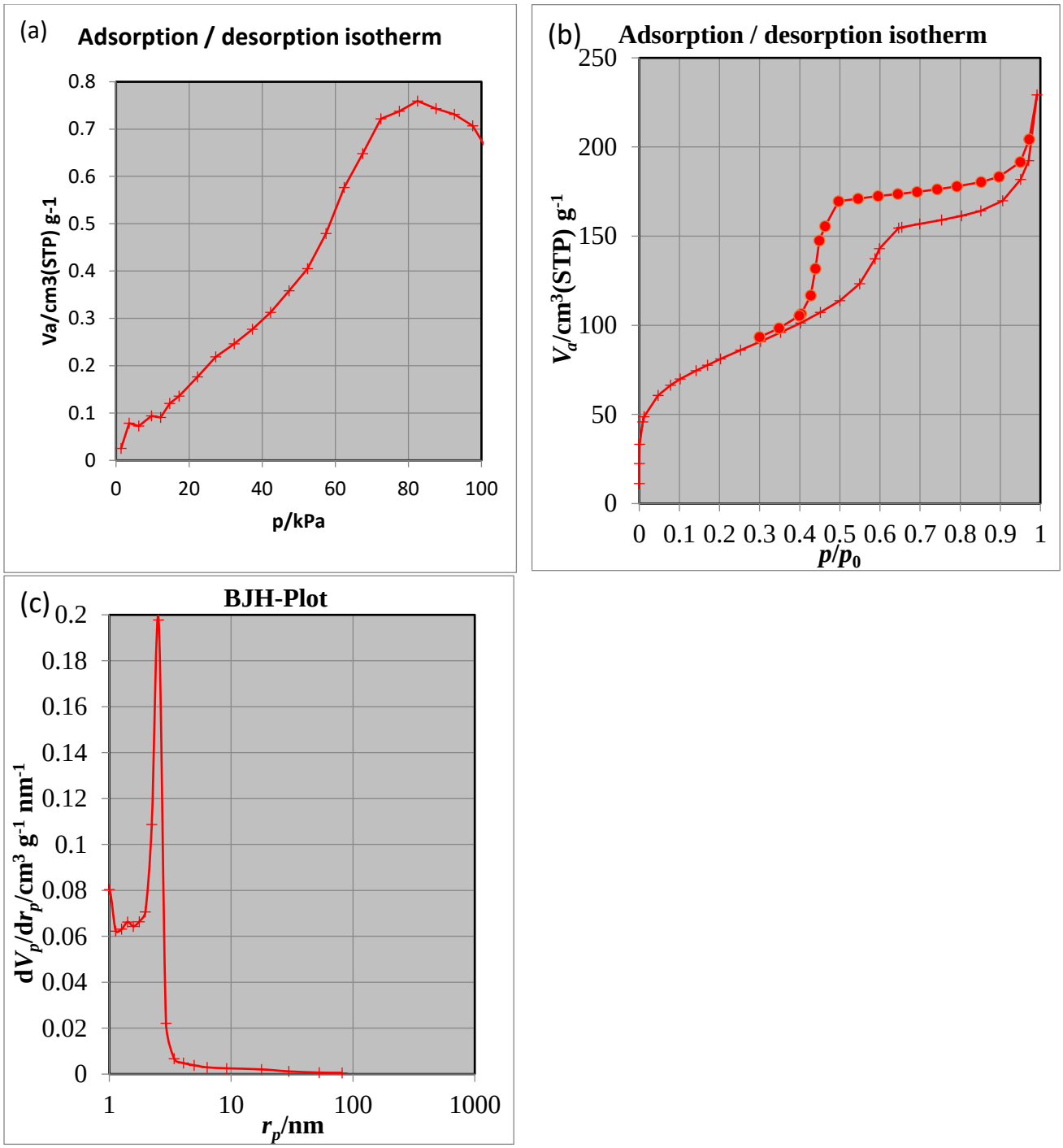


**Fig. 9** $N_2$ adsorption–desorption isotherms for β-CD-bis-APTS (a), $N_2$ adsorption–desorption isotherms for β-CD-APTS-PMO (b) and BJH pore size distributions for β-CD-APTS-PMO (c).

**Table 1** BET surface area, average pore diameter and total pore volume of β-CD-bis-APTS and β-CD-APTS-PMO

| *Nanocarrier* | $a_{s,BET}$ | *Average pore diameter* | $V_m$ |
|---|---|---|---|
| β-CD-bis-APTS | *93.667* | *1.9289* | 12.52 |
| β-CD-APTS-PMO | *284.35* | 4.9301 | *65.33* |
| *Unit* | $[m^2\ g^{-1}]$ | nm | $[cm^3(STP)\ g^{-1}]$ |

**Table 2** Variation of EE (%) and LC (%) with respect to change in nanocarrier amount. Data were expressed as mean ± SDs (n= 3) and inset

| Entry | Nanocarrier | Drug Solution | Drug concentration (µg/ml) | Nanocarrier amount (mg) | LC (%) | EE (%) |
|---|---|---|---|---|---|---|
| 1 | β-CD-bis-APTS | PTX | 500 | 200 | 21.8 ± 0.032 | 43.6 ± 0.64 |
| 2 | β-CD-bis-APTS | PTX | 500 | 250 | 17.76 ± 0.016 | 44.4 ± 0.4 |
| 3 | β-CD-bis-APTS | CUR | 500 | 200 | 23.2 ± 0.014 | 46.4 ± 0.28 |
| 4 | β-CD-bis-APTS | CUR | 500 | 250 | 19.92 ± 0.034 | 49.8 ± 0.85 |
| 5 | β-CD-bis-APTS | CUR/ PTX | 500 / 500 | 200 | 23.0 ± 0.07 /21.4 ± 0.011 | 46.0 ± 0.14 /42.8 ± 0.21 |
| 6 | β-CD-bis-APTS | CUR/ PTX | 500 / 500 | 250 | 19.52 ± 0.021 / 17.12 ± 0.022 | 48.8 ± 0.52 / 42.8 ± 0.55 |
| 7 | β-CD-APTS-PMO | PTX | 500 | 150 | 35.2 ± 0.28 | 52.6 ± 0.42 |
| 8 | β-CD-APTS-PMO | PTX | 500 | 200 | 43.9 ± 0.017 | 87.8 ± 0.34 |
| 9 | β-CD-APTS-PMO | PTX | 500 | 250 | 35.76 ± 0.092 | 89.4 ± 0.23 |
| 10 | β-CD-APTS-PMO | CUR | 500 | 150 | 37.53 ± 0.1 | 56.3 ± 0.37 |
| 11 | β-CD-APTS-PMO | CUR | 500 | 200 | 45.2 ± 0.035 | 90.4 ± 0.71 |
| 12 | β-CD-APTS-PMO | CUR | 500 | 250 | 36.84 ± 0.252 | 92.1 ± 0.63 |
| 13 | β-CD-APTS-PMO | CUR/ PTX | 500 / 500 | 150 | 35.6 ± 0.18 / 33.86 ± 0.24 | 53.4 ± 0.28 / 50.8 ± 0.37 |
| 14 | β-CD-APTS-PMO | CUR/ PTX | 500 / 500 | 200 | 45.1 ± 0.028 / 43.7 ± 0.06 | 90.2 ± 0.56 / 87.4 ± 0.12 |
| 15 | β-CD-APTS-PMO | CUR/ PTX | 500 / 500 | 250 | 36.56 ± 0.064 / 35.24 ± 0.2 | 91.4 ± 0.16 / 88.1 ± 0.52 |

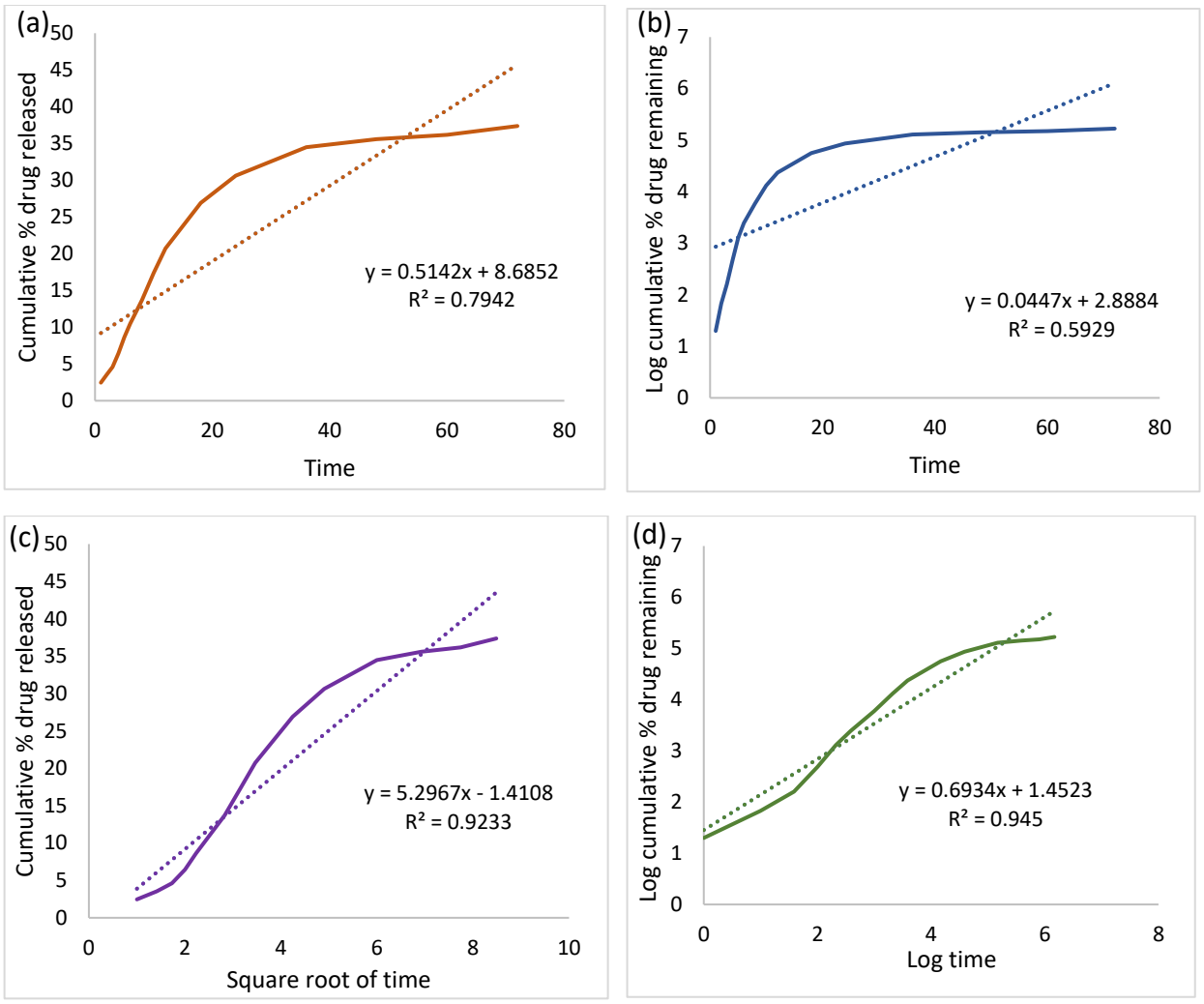


**Fig. 10** Evaluation of mathematical kinetic models for curcumin released from CUR- β-CD-APTS-PMO at pH=7.4: (a) Zero order, (b) First order, (c) Higuchi, and (d) Korsmeyer-Peppas models.

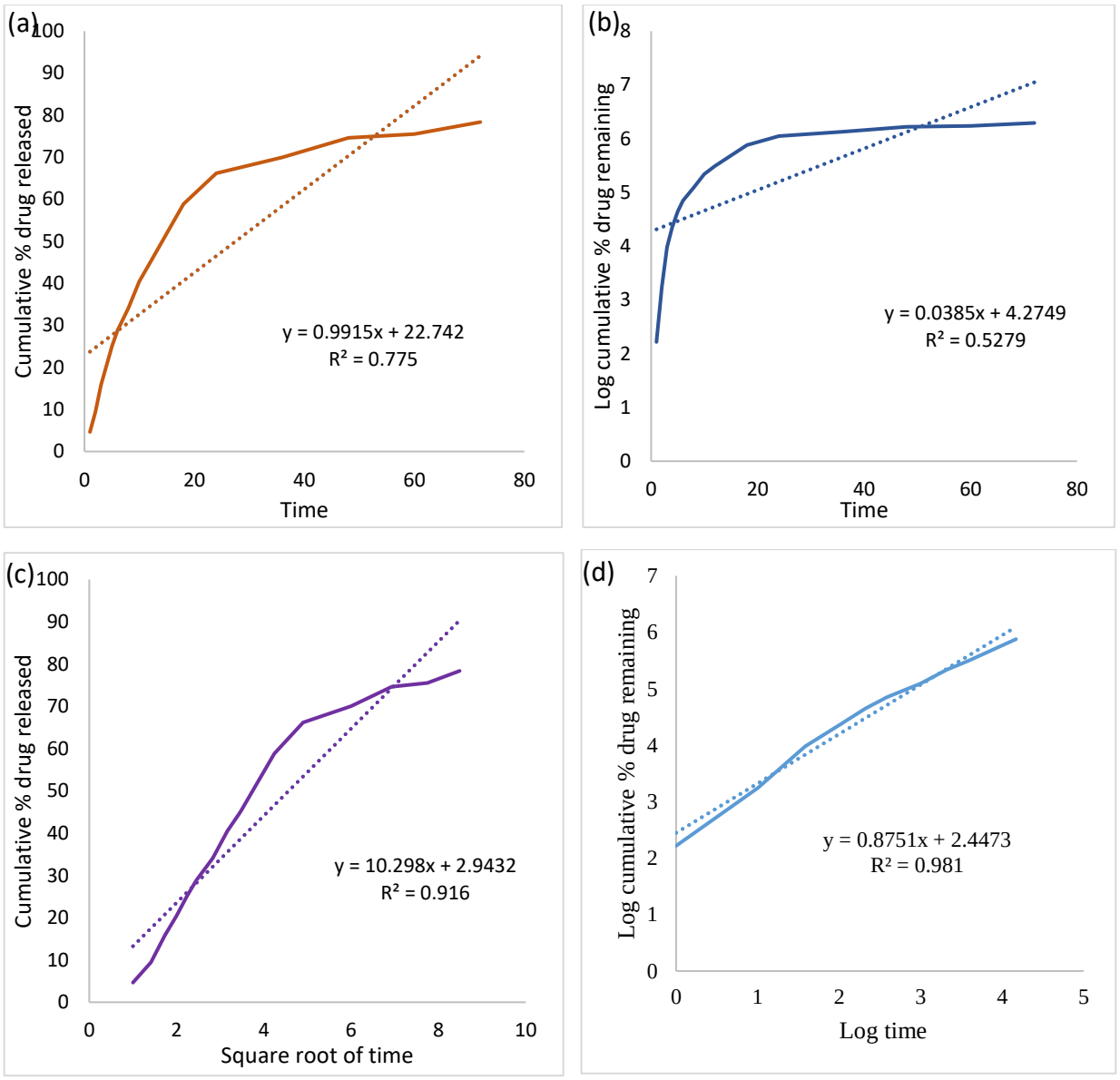


**Fig. 11** Evaluation of mathematical kinetic models for curcumin released from CUR- β-CD-APTS-PMO at pH=5.5: (a) Zero order, (b) First order, (c) Higuchi, and (d) Korsmeyer-Peppas models.

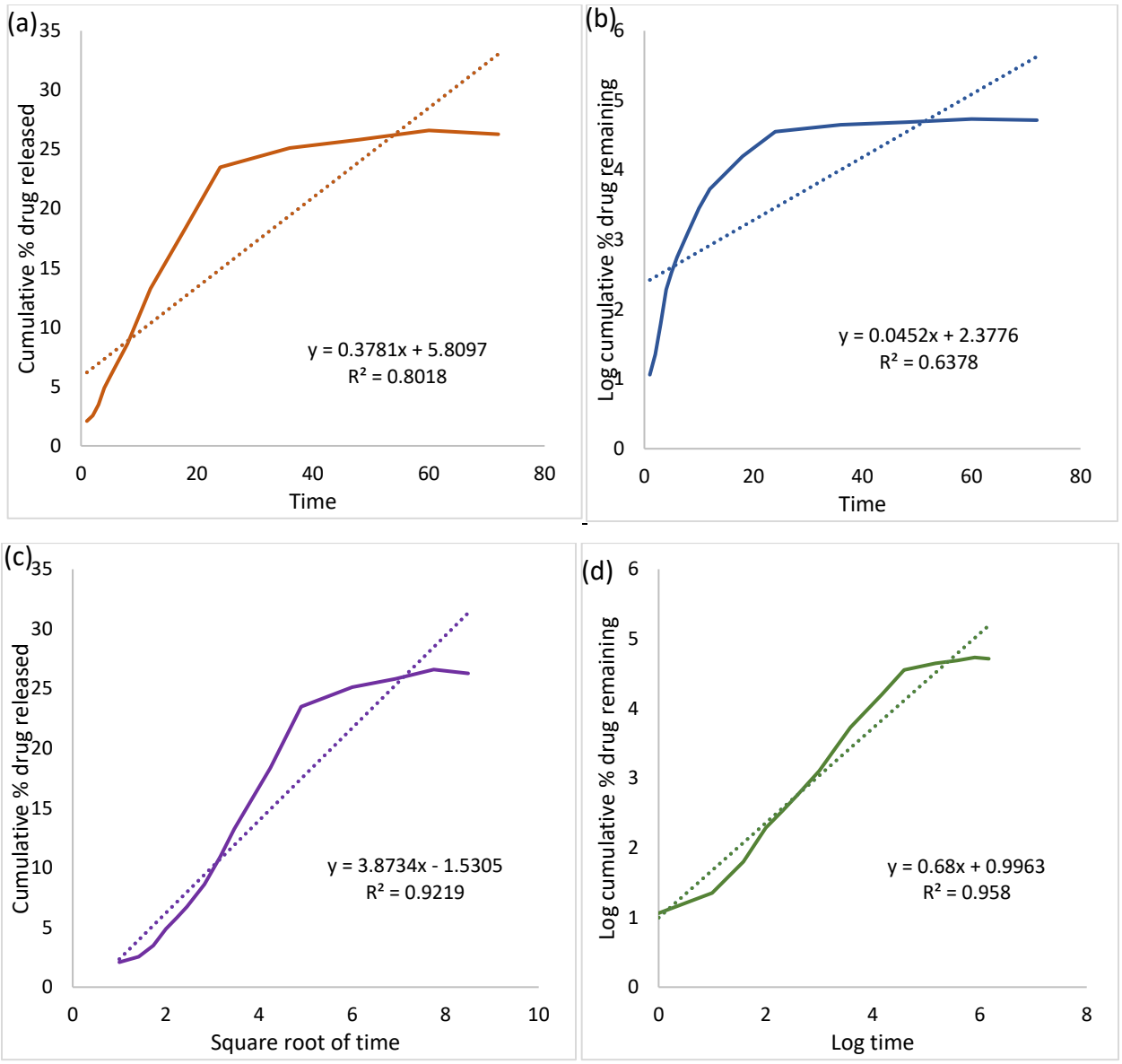


**Fig. 12** Evaluation of mathematical kinetic models for paclitaxel released from PTX-β-CD-APTS-PMO at pH=7.4: (a) Zero order, (b) First order, (c) Higuchi, and (d) Korsmeyer-Peppas models.

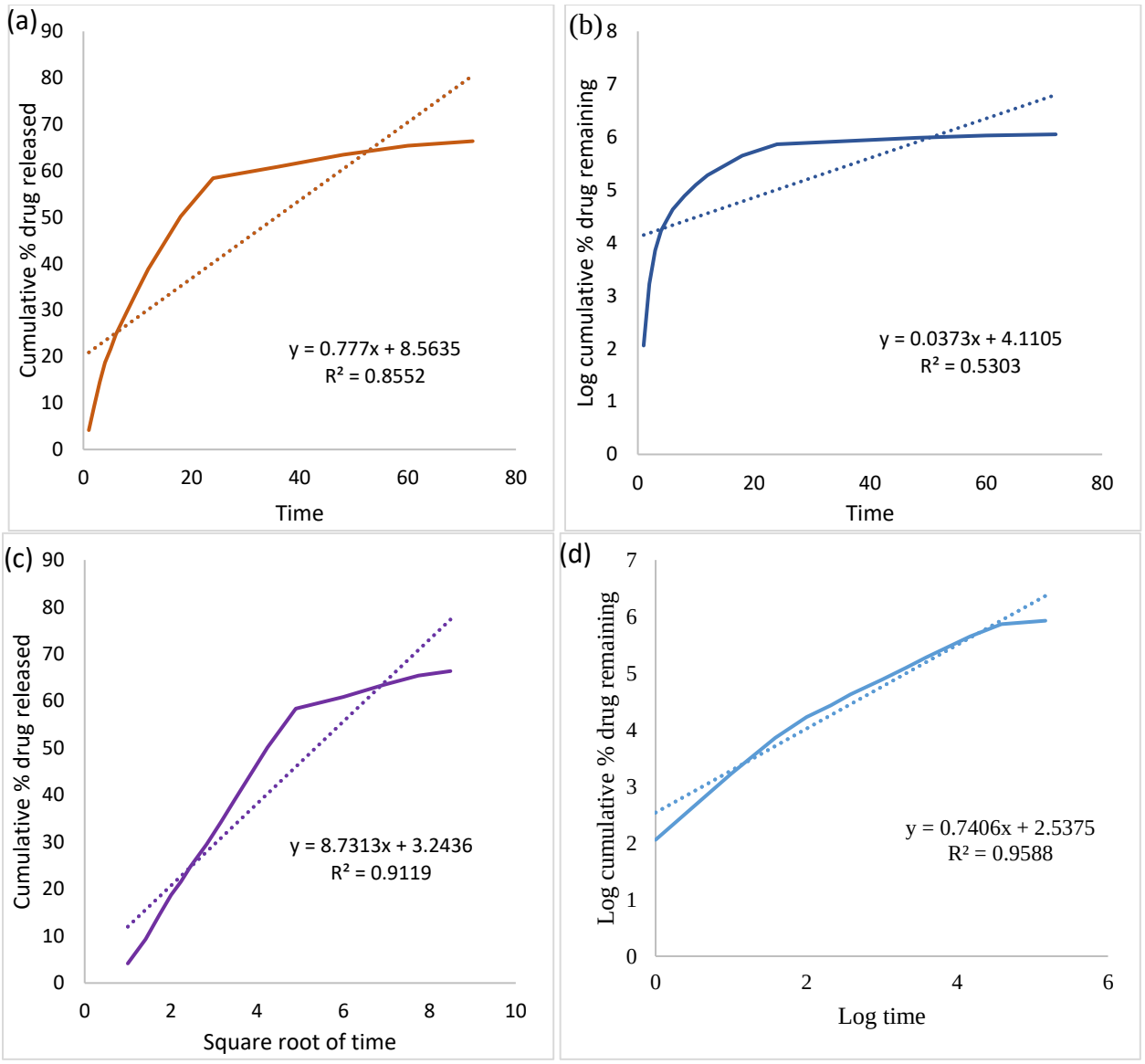


**Fig. 13** Evaluation of mathematical kinetic models for paclitaxel released from PTX-β-CD-APTS-PMO at pH=5.5: (a) Zero order, (b) First order, (c) Higuchi, and (d) Korsmeyer-Peppas models.

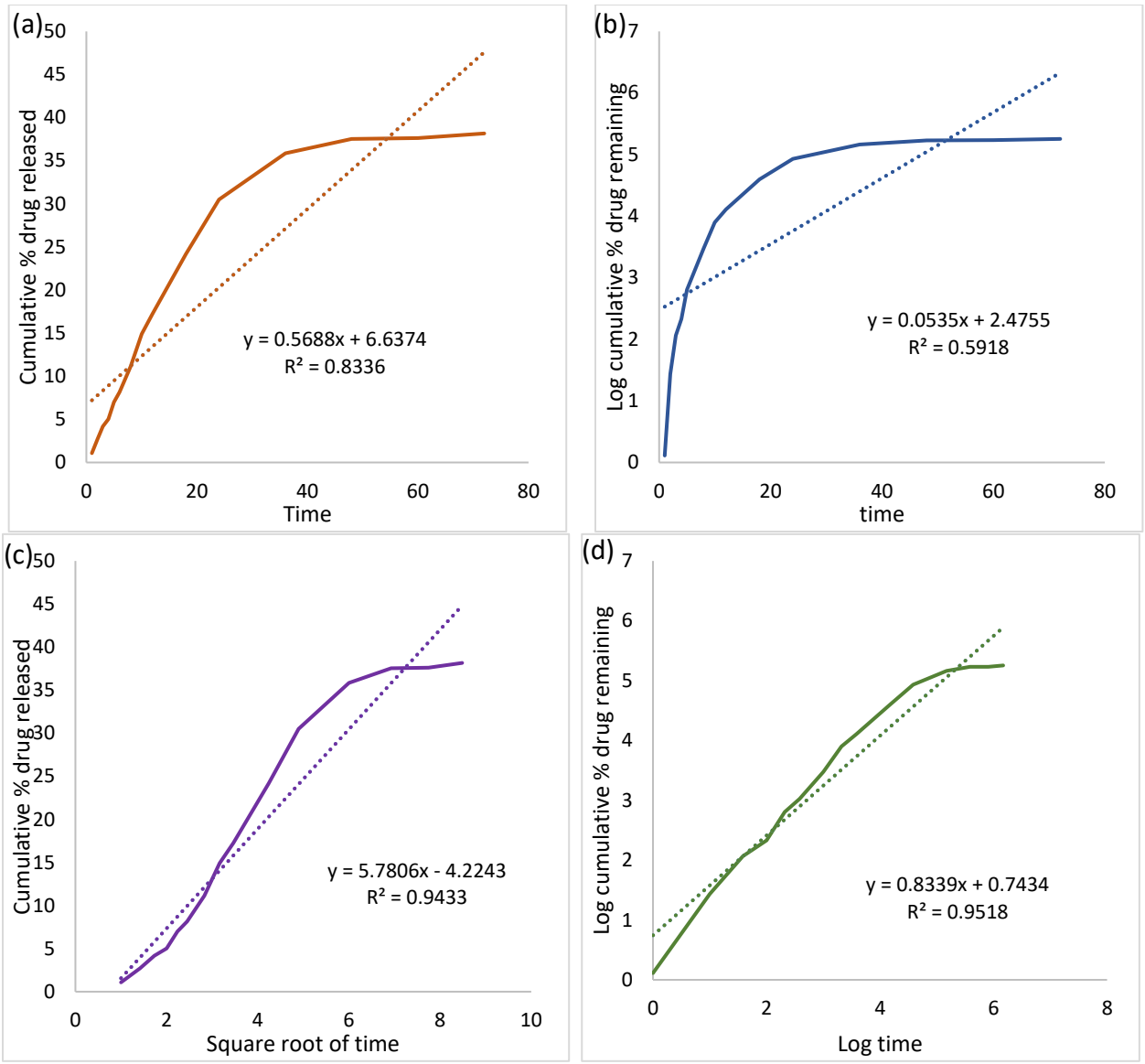


**Fig. 14** Evaluation of mathematical kinetic models for curcumin released from PTX/CUR-β-CD-APTS-PMO at pH=7.4: (a) Zero order, (b) First order, (c) Higuchi, and (d) Korsmeyer-Peppas models.

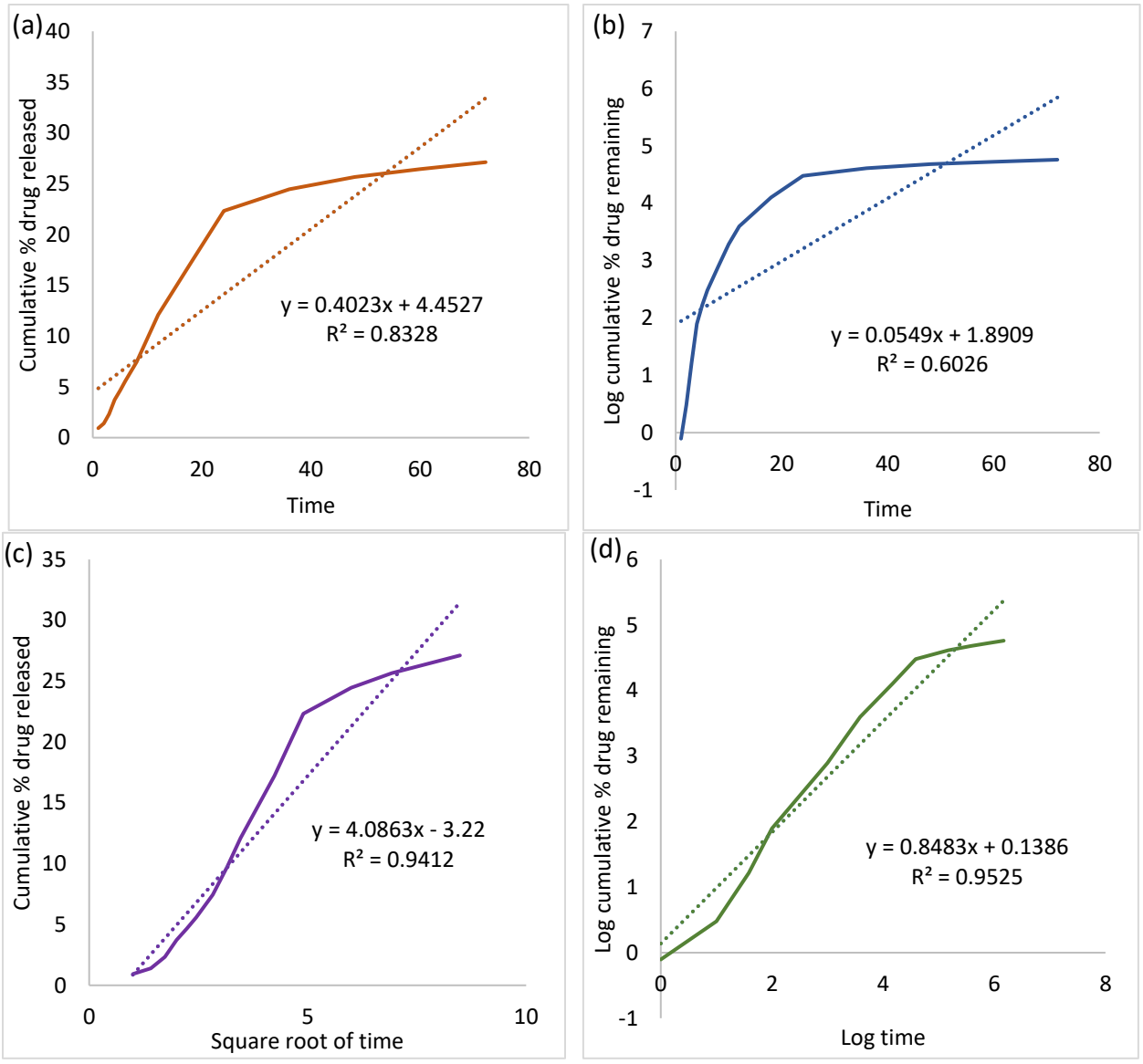


**Fig. 15** Evaluation of mathematical kinetic models for paclitaxel released from PTX/CUR-β-CD-APTS-PMO at pH = 7.4: (a) Zero order, (b) First order, (c) Higuchi, and (d) Korsmeyer-Peppas models.

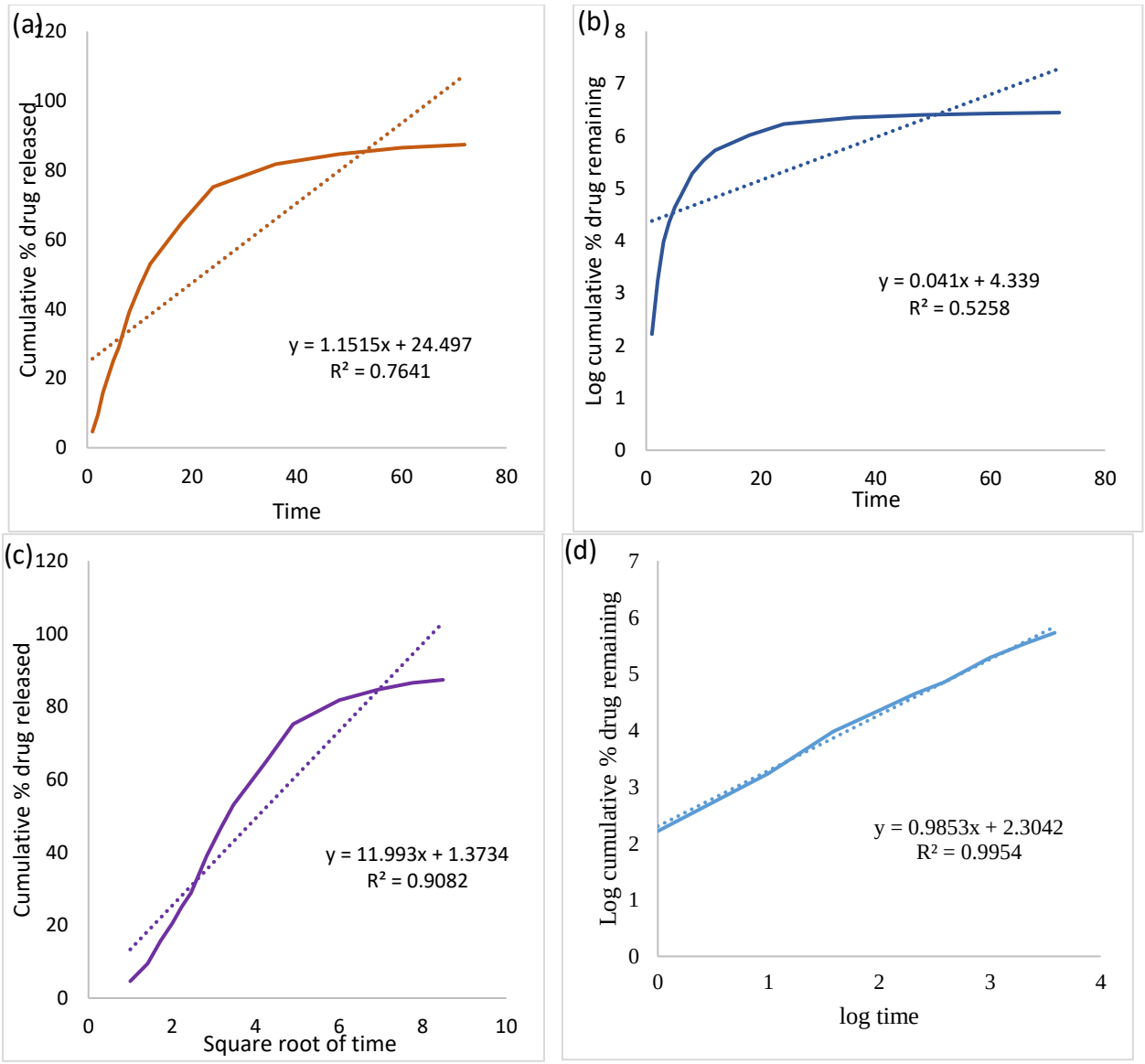


**Fig. 16** Evaluation of mathematical kinetic models for curcumin released from PTX/CUR-β-CD-APTS-PMO at pH = 5.5: (a) Zero order, (b) First order, (c) Higuchi, and (d) Korsmeyer-Peppas models.

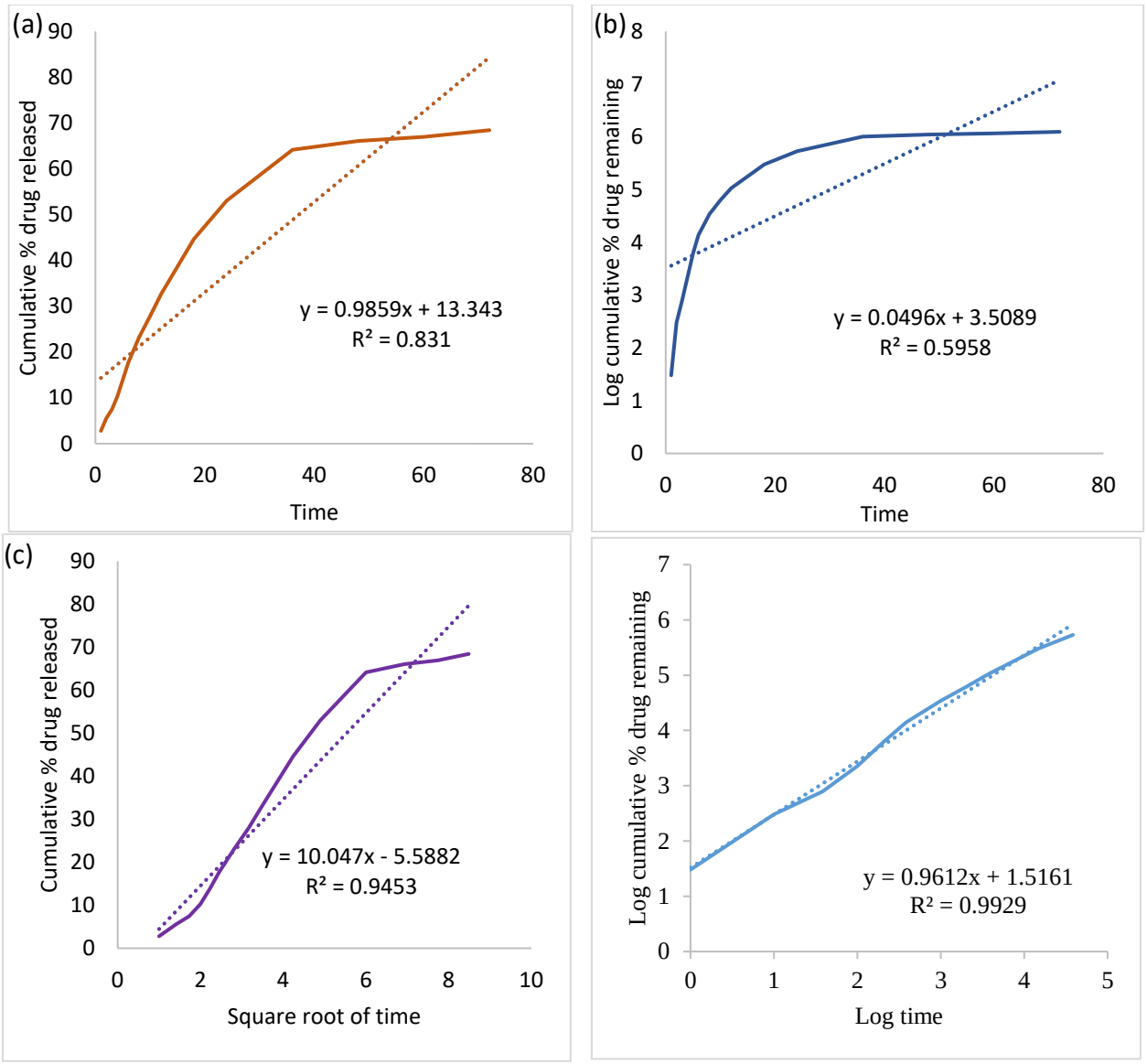


**Fig. 17** Evaluation of mathematical kinetic models for paclitaxel released from PTX/CUR-β-CD-APTS-PMO at pH = 5.5: (a) Zero order, (b) First order, (c) Higuchi, and (d) Korsmeyer-Peppas models.

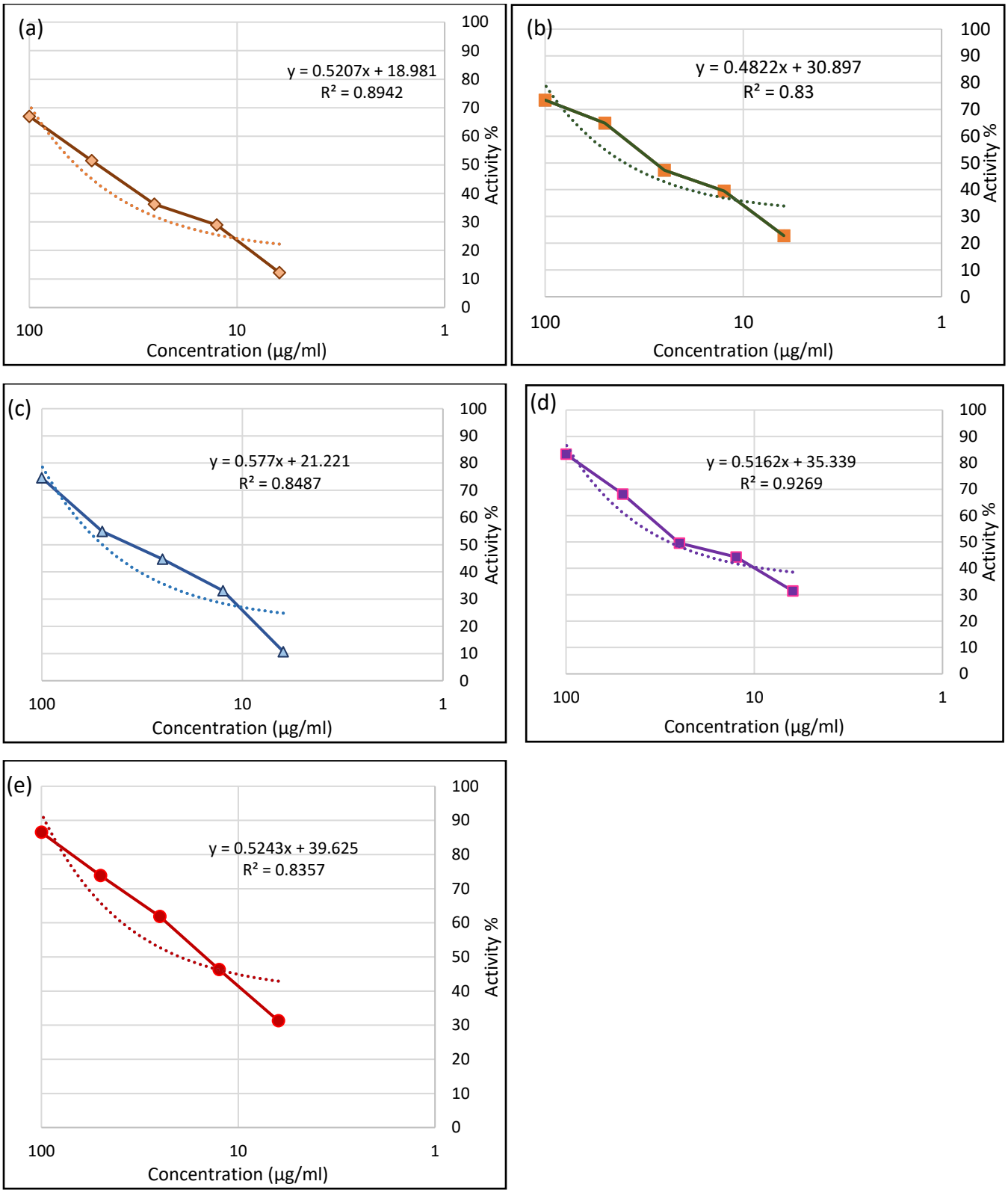


**Fig. 18** IC50 curve of pure curcumin (a), paclitaxel (b) and CUR-β-CD-APTS-PMO (c) PTX-β-CD-APTS-PMO (d) PTX/CUR-β-CD-APTS-PMO (e).